Title

Reliability of Semiautomated Kinetic Perimetry (SKP) and Goldmann Kinetic Perimetry in Children and Adults With Retinal Dystrophies.

Journal

Translational vision science & technology, 8(3)

ISSN

2164-2591

Authors

Barnes, Claire S
Schuchard, Ronald A
Birch, David G
et al.

Publication Date

2019-05-01

DOI

10.1167/tvst.8.3.36

Peer reviewed

tvst

https://doi.org/10.1167/tvst.8.3.36

Article

Reliability of Semiautomated Kinetic Perimetry (SKP) and Goldmann Kinetic Perimetry in Children and Adults With Retinal Dystrophies

Claire S. Barnes[1], Ronald A. Schuchard[2], David G. Birch[3], Gislin Dagnelie[4], Leah Wood[5], Robert K. Koenekoop[6], and Ava K. Bittner[4,7,8]

[1] Palo Alto, CA, USA
[2] Envision Research Institute, Wichita, KS, USA
[3] Retina Foundation of the Southwest, Dallas, TX, USA
[4] Department of Ophthalmology, Johns Hopkins University, Baltimore, MD, USA
[5] Department of Ophthalmology and Visual Sciences, Dalhousie University, Halifax, Canada
[6] Department of Ophthalmology, McGill University Health Centre, Montreal, Canada
[7] Nova Southeastern University, College of Optometry, Fort Lauderdale, FL, USA
[8] Department of Ophthalmology, Stein Eye Institute, University of California, Los Angeles, Los Angeles, CA, USA

Correspondence: Claire S. Barnes, 4274 Wilkie Way, Palo Alto, CA 94306, USA. e-mail: Claire_Barnes@att.net

Received: 15 November 2018
Accepted: 7 April 2019
Published: 11 June 2019

Keywords: semiautomated kinetic perimetry (SKP); Goldmann perimetry; retinitis pigmentosa; Leber congenital amaurosis; test–retest variability; children

Citation: Barnes CS, Schuchard RA, Birch DG, Dagnelie G, Wood L, Koenekoop RK, Bittner AK. Reliability of semiautomated kinetic perimetry (SKP) and Goldmann kinetic perimetry in children and adults with retinal dystrophies. Trans Vis Sci Tech. 2019;8(3):36, https://doi.org/10.1167/tvst.8.3.36

Purpose: To investigate the precision of visual fields (VFs) from semiautomated kinetic perimetry (SKP) on Octopus 900 perimeters, for children and adults with inherited retinal degenerations (IRDs). Goldmann manual kinetic perimetry has long been used in the diagnosis and follow-up of these patients, but SKP is becoming increasingly common. Octopus VFs (OVFs) and Goldmann VFs (GVFs) were both mapped on two occasions.

Methods: Nineteen females and 10 males with IRDs were tested on OVFs and GVFs, with two targets per test (V4e and one smaller target). Tests were performed in the same (randomized) order at two visits about 1 week apart. The VFs were digitized to derive isopter solid angles. Comparisons, within and between visits, were performed with paired *t*-tests and Bland-Altman plots.

Results: Median age was 20 years (range, 7–70; 10 participants aged $\leq$17 years old). There were no significant differences in solid angles between OVFs and GVFs ($P \geq 0.06$) or between the two visits' solid angles on either perimeter ($P \geq 0.30$). Between-visit test–retest variability for GVFs and OVFs was similar ($P \geq 0.73$), with median values of approximately 9% to 13%. Overall variability was lower for children than adults (medians of 7.5% and 12.8%, respectively).

Conclusions: Octopus SKP and Goldmann perimetry produced VFs of similar size and variability.

Translational Relevance: Our study indicates that SKP provides a viable alternative to traditional Goldmann perimetry in clinical trials or care involving both children and adults with IRDs.

Introduction

The Goldmann perimeter has long been considered the "gold standard" for mapping the visual fields (VFs) of patients with inherited retinal degenerations (IRDs),[1,2] both for aiding in diagnoses and for tracking disease progression. Advantages of Goldmann perimetry are that (1) it allows the mapping of the far periphery of the VF, which may have residual "islands" of function; (2) it allows for close investigation of small VF regions and dense scotomas[3]; and (3) the operator is closely engaged with the patient during the test, including monitoring the patient's fixation.[4] An experienced Goldmann operator, thus,

can help the patient stay attentive to the test, which is especially helpful when testing children.[2,4]

With Goldmann perimeters no longer in production,[2] other kinetic and hybrid perimeters, such as the Octopus 900 (Haag Streit AG, Koeniz, Switzerland), are increasingly used to obtain detailed VFs. The Octopus 900 can be used for "semiautomated kinetic perimetry" (SKP),[3] as opposed to the manual kinetic technique on Goldmann perimeters. It is thought that kinetic VF testing could be standardized with SKP[3] because the target velocities (speed of target movement from nonseeing to seeing retina) can be fixed for each vector and because the same starting test pattern can be used across repeat tests. Minimizing VF variability (i.e., differences in responses across repeat tests for a given individual) is the key to identifying genuine changes in visual function over time to document true disease progression or positive treatment effects. An additional advantage of the Octopus perimeter is that it calculates the squared-degrees (deg^2) values for each isopter,[5] without the need for manual–measuring or –digitizing, so that VF sizes can quickly be quantified for comparison across successive visits.

There have now been a number of studies published regarding Octopus SKP, but there are some gaps in the literature. For example, studies with direct comparisons between Octopus and Goldmann perimetry are still scarce, particularly in terms of test–retest variability per instrument. Same-day comparisons of Octopus visual fields (OVFs) and Goldmann visual fields (GVFs) in glaucoma patients showed "generally good agreement,"[6] with results in mixed groups of patients and control subjects showing trends to OVF areas being slightly larger than the corresponding GVF areas, particularly for small and/or dim targets.[2,3,6,7] We are aware of only one study[8] in which both GVFs and OVFs were measured on two different days on the same participants, but the focus of that study was on the feasibility of testing visually normal children with SKP, and the isopter areas and variabilities were not directly compared between the two types of perimeters.

Furthermore, although there have been multiple SKP studies that tested adult patients with retinal[5,9–11] or neurological disorders,[12] as well as adult control subjects,[1,13] there have been few studies of SKP in children. Specifically, we know of only four pediatric studies on SKP or automated kinetic perimetry.[1,4,8,14] Primarily, though, those studies tested visually normal children or tested the unaffected eye of children with monocular eye disorders. Nowomiejska et al.[15] tested a 16-year-old participant in their Leber hereditary optic neuropathy study, and Nasser et al.[16] tested 3 children (ages 7 to 17 years old; only the oldest had a "recordable" VF) as part of their characterization of patients with Alström syndrome. It is important to determine whether Octopus SKP is feasible and reliable in fairly young children (e.g., over age 5 years) with IRDs. The present study was designed to record OVFs and GVFs in both children and adults with IRDs to compare isopter sizes (solid angles) and to examine the test–retest variability (precision) for the two types of perimeters. This information will be of assistance for planning IRD clinical trials that use VFs as an outcome measure and will also be of clinical relevance for documenting disease progression as Octopus perimeters continue to replace Goldmann perimeters.

Methods

Participants

The study was performed at the Retina Foundation of the Southwest (10 participants), Montreal Children's Hospital at McGill University (10 participants), and the Wilmer Eye Institute (9 participants). Institutional Review Board approval for the study was obtained at each site. Informed consent (and assent, as applicable) was obtained from each participant before any testing was performed, and the protocol followed the tenets of the Declaration of Helsinki. Children (age $\geq$6 years) and adults with an established IRD diagnosis (with or without an identified mutation), but with no other disorder affecting vision, were enrolled. Participants had decreased VFs, ideally such that their central VF measured with the V4e target was between 10 and 60 degrees in diameter in both eyes, with or without peripheral islands of vision.

Procedure

Monocular visual acuities were measured with the Early Treatment Diabetic Retinopathy Study chart at participants' first data-collection visit (Visit 1) or were obtained from recent ophthalmic records.

One assessment on an Octopus 900 perimeter (Haag Streit AG) and one assessment on a Goldmann perimeter were completed at each of two visits, approximately 1 week apart. The median time between visits was 7 days and the range was 2 to 20 days. The order in which the perimeters were to be tested was randomized at the first visit, and the same

order was followed at the second visit. One eye of each participant was tested: either the eye with better visual acuity or, if the acuities were equal, the participant's preferred eye. During testing, the non-study eye was covered with an eye-patch. Each participant was tested with the V4e target and one smaller target. The smaller target was chosen by the operator with the intention that, at 4e intensity, the resultant isopter would be approximately 10 degrees in diameter.

Participants adjusted to the dim study-room lighting for 10 minutes before each test. The background luminance on both perimeters was set at 31.4 apostilb. Target speed on the Octopus 900 was set at 4 deg/s, except for the mapping of scotomas or small seeing regions, for which the speed was reduced to 2 deg/s. The target speed for GVF mapping was approximately 4 to 5 deg/s, which is consistent with an earlier estimate,[2] with slower target movements used for the mapping of small seeing or nonseeing regions. The target vectors were mapped at meridians every 15 degrees, for both target sizes on both perimeters.

Following the OVF mapping, reaction times were recorded on the Octopus. The reaction time (in milliseconds) was the average, across six trials, of the time needed for the participant to push the button following the onset of the target moving within their seeing field (typically placed in the central field). The target speed was 4 deg/s for the reaction-time tests.

All VF testing for a given participant was performed by the same examiner to eliminate interexaminer differences as one possible source of variability.[17] All examiners were highly experienced with Goldmann perimetry for patients with IRDs. Participants were encouraged to take as many breaks as necessary. During the perimetry, examiners frequently assessed participants for factors that could affect test outcome, specifically fixation, fatigue, cooperation, and photopsias. Afterward, the examiners rated subjects on each factor, on a scale from 5 (no problem noted or reported) to 1 (such a problem that isopter mapping could not be completed).

Analysis

VF area is a commonly used clinical measure. However, whereas area measures near the center of a VF chart closely represent both solid angles and retinal areas, at more peripheral locations, the flat chart exaggerates the area of chart regions, relative to the corresponding area on a sphere (the solid angle) or in the eye. As such, solid angles are less sensitive to peripheral distortions than are area measures.[18] The VF solid angles (in steradians, "sr") in this study were derived by on-screen digitizing of the scanned OVFs and GVFs by using the FieldDigitize v4.0 program.[18–20] All digitizing was performed by the same person. The OVF solid angles from the digitizing software were also compared with the deg^2 values directly generated by the Octopus perimeters for the same isopters.

Summaries for continuous variables included the sample size, median, and range. Summaries for discrete variables included frequencies and percentages. The data analyses primarily focused on (1) the within-visit comparison between GVFs and OVFs, in terms of the similarity in solid angles; and (2) the across-visit test–retest variability for each method (e.g., Visit 1 GVF versus Visit 2 GVF). Two-tailed (alpha = 0.05) paired *t*-tests and Bland-Altman regression plots were used to compare results within and between visits. If a data point in any paired *t*-test was missing, then the corresponding point for the other test was excluded. For example, there was an error in mapping the smaller OVF isopter for participant C4 at the second visit, so the corresponding isopter from the first visit was excluded from relevant *t*-tests. To not overestimate the degrees of freedom or to underestimate the standard deviations, and thereby derive artificially low *P* values, averages across the two visits were performed prior to the *t*-tests for comparing the solid angles between the two perimeters. As there were relatively few participants tested with each of the smaller targets (I4e to IV4e), the data were merged into a "smaller target" group for analysis.

Test–retest variability was calculated as a percentage, using the following equation:

$$\text{Test} - \text{retest variability} = \frac{\text{Absolute value of}(\text{Visit 1 VF} - \text{Visit 2 VF})}{\text{Average of}(\text{Visit 1 VF} + \text{Visit 2 VF})} \times 100.$$

Results

Demographics

Twenty-nine participants (19 females and 10 males) were enrolled across the three sites. Demographic characteristics for the participants at each site are summarized in Table 1 (full details for individual participants are provided in Supplementary Table S1). The participants ranged in age from 7 to 70 years

Table 1. Participant Demographics by Site

Site	Number of Participants (Females; Males)	Range of Ages, Years (Median)	Range of Visual Acuities (Snellen)[a]	Range of Visual Acuities, Snellen Equivalent logMAR (Median)
A	10 (5; 5)	10 to 70 (16.5)	20/32 to 20/320	0.20 to 1.20 (0.45)
B	10 (5; 5)	14 to 52 (30.5)	20/20 to count fingers[d]	0.0 to 1.85 (0.3)
C	9 (9; 0)	7 to 39 (18)	20/19 to 20/46	−0.02 to 0.36 (0.1)

[a] The visual acuity values for the participants at site B were taken from the charts, not measured at the study visits. Visual acuities for the participants at the other two sites were measured at their first study visit.

[b] USH II, Usher syndrome II; CRD, cone-rod dystrophy; LCA, Leber congenital amaurosis; RP, retinitis pigmentosa. Where known, the LCA gene mutation has been noted: RDH12, retinol dehydrogenase 12; CRB1, Crumbs 1.

[c] Perimetry targets used in addition to the V4e target.

[d] The conversion to logMAR for count fingers was based on Schulze-Bonsel et al.[22]

Table 1. Extended

Site	Diagnoses[b]	Intervals between Visits, Days (median)	Smaller Visual Field Targets Tested Per Site[c]
A	one USH II; two LCA; two CRD; five RP	2 to 20 (6)	one I4e; one II4e; seven III4e; one IV4e
B	five RP; five LCA (one RDH12, three CRB1)	4 to 7 (7)	three I4e; three II4e; three III4e; one IV4e
C	nine RP	6 to 9 (7)	four I4e; three III4e; one IV4e; one N/A

(median = 20 years). The study included 10 children (7–17 years, inclusive); 15 participants were <24 in age (i.e., children and "young people," according to the World Health Organization[21]). There were 19 participants with retinitis pigmentosa, 7 with Leber congenital amaurosis, 2 with cone-rod dystrophy, and 1 with Usher syndrome II. The visual acuity values for the test eyes ranged from 20/19 Snellen to "count fingers" (based on Schulze-Bonsel et al.,[22] the participants with count fingers visual acuity were assigned a log of the minimum angle of resolution [logMAR] value of 1.85).

Two of the participants (A8 and B1) had OVFs that were too small to reliably digitize; their V4e isopter diameters were about 5 degrees, with the symbols so thoroughly overlapping that the isopter edges could not be distinguished. For participant B1, the smaller-target (III4e) *GVF* isopters at both visits were also too small to digitize, so participants A8 and B1 were not included in the quantitative analyses. Without those 2 participants, there were 9 children and 18 adults in the study (8 males), with a median age of 23 years. Finally, one of the participants (C2) was only tested with the V4e target due to her feeling unwell at Visit 1 (so only V4e was tested at Visit 2 also), and the OVFs of the smaller targets were missing at Visit 2 for two participants (A4 and C4) because of errors in the testing or mapping. In total, therefore, there were 54 V4e isopters for each perimeter and 52 GVF and 50 OVF smaller-target isopters digitized in this study.

Figure 1 displays results that are similar between VF tests, for one participant. In Figure 1, the GVFs (panels A and C) are similar in general size and shape for the two visits. The two GVFs for this participant are also similar to the corresponding OVFs (panels B and D). The solid angle values for the individual panels and the calculated variabilities across test conditions confirm the qualitative assessment of similarity. Conversely, the OVFs and GVFs in Supplementary Figure S1 are generally less similar.

Comparisons Within Goldmann Perimetry and Octopus SKP, Between Visits

A summary of the VF solid angles, by target size, perimetric method, and visit number is presented in Table 2. The study participants displayed a wide range of VF sizes for the V4e target and for the smaller targets.

Scatterplots of the Visit 2 solid angles against the Visit 1 solid angles, for each perimetric method and target size, are presented in Figure 2. All results fell

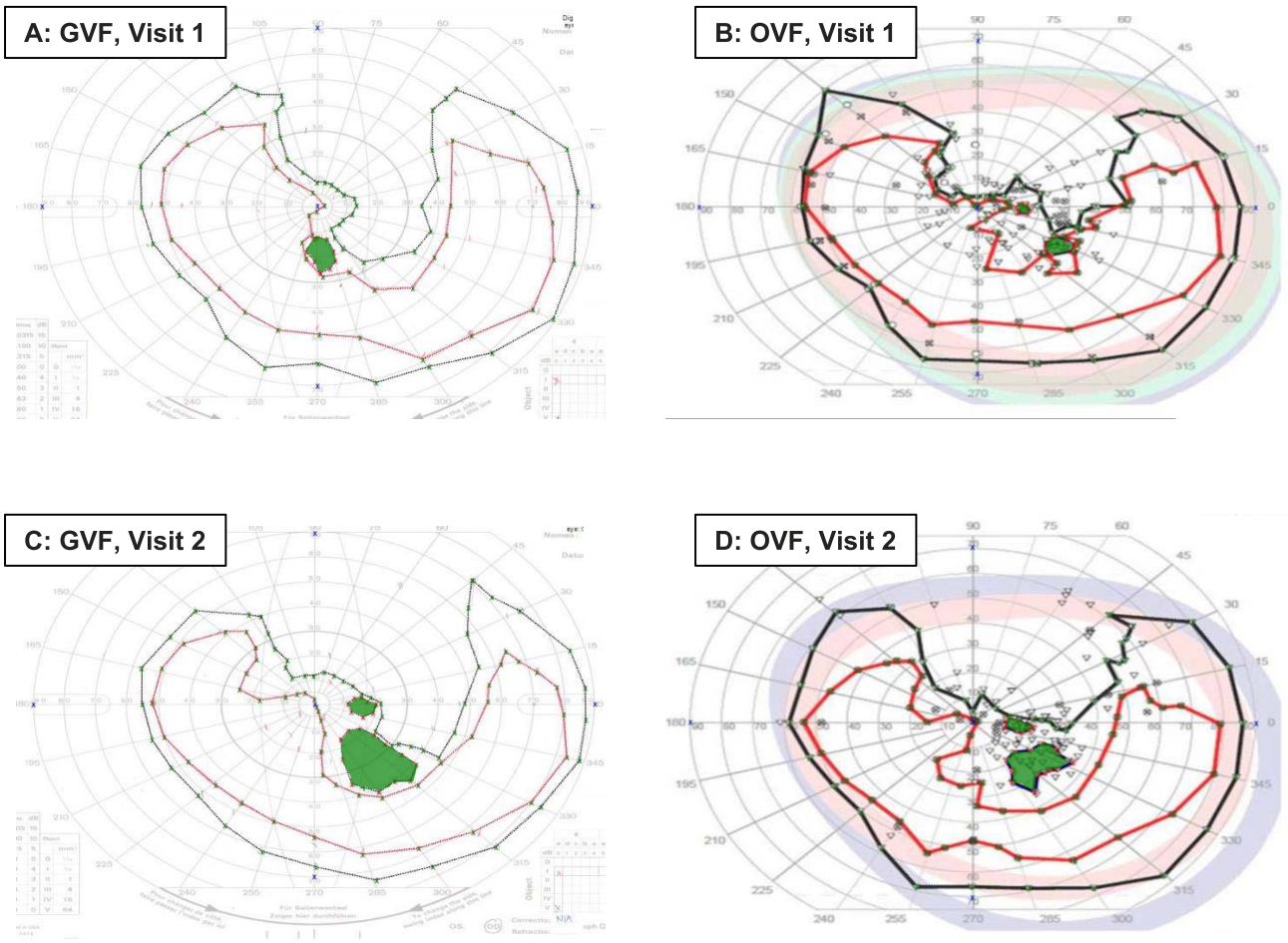

	Participant B4: Visual Field Solid Angles (sr)			
	GVF V4e	OVF V4e	GVF I4e	OVF I4e
Visit 1	2.81	2.71	1.68	1.60
Visit 2	2.56	2.70	1.52	1.24

	Participant B4: Test-Retest Variability for Solid Angle Measures (%)			
	GVF Visit 1 vs. Visit 2	OVF Visit 1 vs. Visit 2	GVF vs. OVF Visit 1	GVF vs. OVF Visit 2
V4e	9.16	0.333	3.70	-5.13
I4e	9.70	25.2	4.83	20.4

Figure 1. Example of similar GVFs and OVFs from participant B4. Each panel shows the isopter for the I4e target (inner ring), and the isopter for the V4e target (outer ring). V4e scotomas are *shaded*. Note the similarity in the size and shape within each type of test between Visits 1 and 2 (A versus C and B versus D, for GVFs and OVFs, respectively) and between tests for the two perimeters on each visit (A versus B for Visit 1, and C versus D for Visit 2). The corresponding numerical results are shown in the tables.

close to the identity line (y = x; solid line), and there was good correlation between the Visit 1 and Visit 2 solid angles for both perimetric methods and for both the V4e isopter and the smaller-target isopters (r^2 values between 0.93 and 0.95, as shown on each panel).

Across participants, the solid angles were not significantly different between visits for either GVFs or OVFs and for either V4e targets or smaller targets. The *P* values for the paired *t*-tests within test conditions comparing Visit 1 to Visit 2 were the

Table 2. GVF and OVF Solid Angles, by Perimetric Method and Visit Number

Target Size	Parameter	Visual Field Solid Angles (sr)			
		Visit 1		Visit 2	
		GVF	OVF	GVF	OVF
V4e	*n*	27	27	27	27
	Median	1.89	1.66	1.81	1.69
	Minimum	0.027	0.025	0.045	0.020
	Maximum	3.94	4.04	3.79	3.97
Smaller targets	*n*	26[a]	26[a]	26[a]	24[b]
	Median	0.29	0.32	0.29	0.38
	Minimum	0.017	0.013	0.017	0.012
	Maximum	2.66	2.80	2.66	2.89

[a] Participant C2 was only tested with the V4e target.
[b] Participants A4 and C4 had no smaller-target data for their second visit, due to errors in mapping.

following: V4e GVFs, $P = 0.33$; V4e OVFs, $P = 0.30$; smaller-target GVFs, $P = 0.90$; and smaller-target OVFs, $P = 0.71$.

Comparisons Between Goldmann Perimetry and Octopus SKP, Within Visits

The solid angles measured from the OVFs, graphed against the GVF solid angles at the same visit, are presented in Figure 3. The solid line in each graph is the identity line (y = x). The results from the two perimeters were similar within Visit 1 and within Visit 2.

The solid angles for the V4e isopters mapped with SKP were very similar to those from Goldmann perimetry, both within each visit and for the two visits combined ($r^2 = 0.93$ and 0.95 for Visits 1 and 2, respectively; $r^2 = 0.94$, y = 1.001x + 0.029 for the combined-visit data). Results of the OVFs and GVFs for the smaller-target isopters were only slightly less

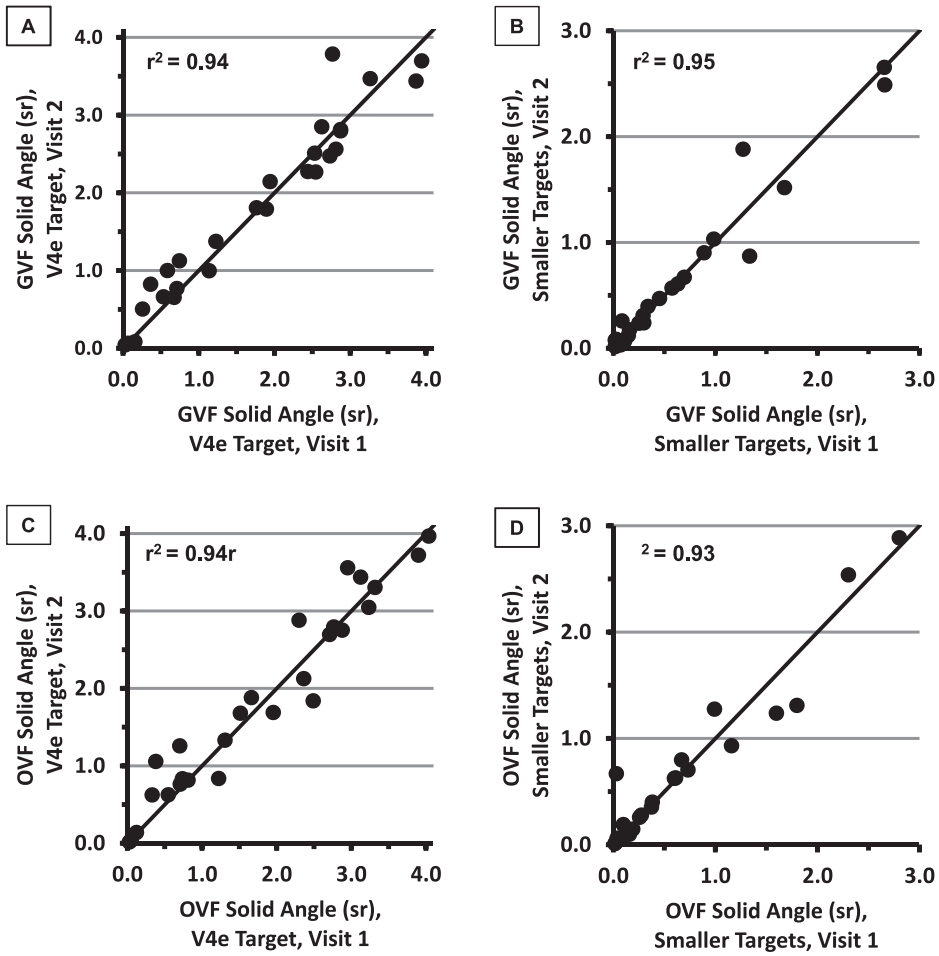

Figure 2. Visual field solid angles at Visit 1 (x-axes) and Visit 2 (y-axes) for GVFs (A and B) and OVFs (C and D), for V4e targets (panels A and C) and for the smaller targets (panels B and D).

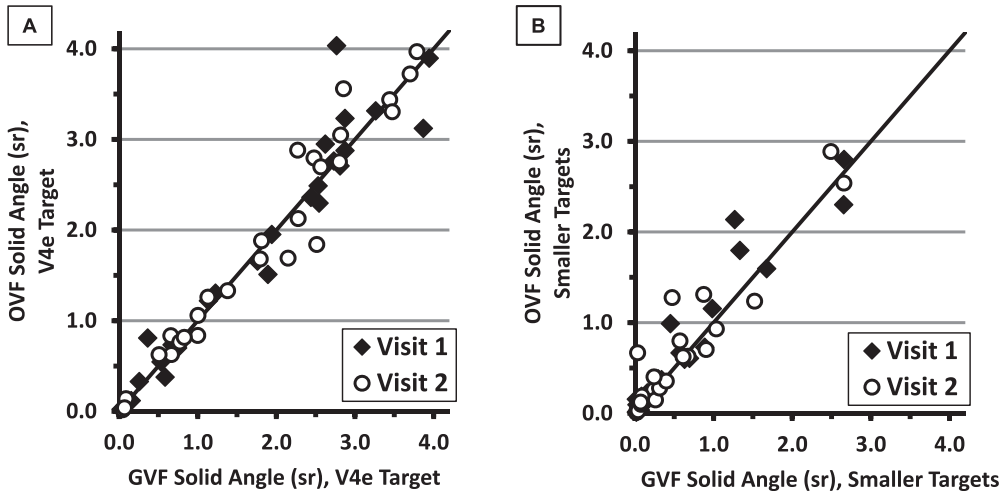

Figure 3. Solid-angle measures for OVFs versus GVFs for the V4e target (A) and for the smaller targets (B). Values from the first visit are represented by the *filled diamonds* and those from the second visit by the *open circles*. The *solid lines* indicate equal values for the OVF and GVF solid angles.

similar (r^2 = 0.91 and 0.89 for Visits 1 and 2, respectively; r^2 = 0.90, y = 0.994x + 0.085 for the combined-visit data). There were no statistically significant differences in the averaged isopter sizes (per participant) between-visits when comparing the OVFs and GVFs for the V4e targets ($P = 0.48$, 27 pairs) or for the smaller targets ($P = 0.06$, 26 pairs).

Comparisons Between Goldmann Perimetry and Octopus SKP Test–Retest Variability

Test–retest variability results for the two perimeters are presented in Table 3, first for all participants combined, and then separately for the groups of pediatric and adult participants.

For the full set of participants, the median test–retest variabilities were 9.7% for GVFs with the V4e target and 8.7% for GVFs with the smaller targets. The median test–retest variabilities for OVF solid angles were fairly similar to those for GVFs, at 12.7% for the V4e target and 8.9% for the smaller targets. Paired *t*-tests between the GVF and OVF test–retest variabilities for the V4e targets and, separately, for the smaller targets showed no significant differences in the variabilities for the two perimeters ($P = 0.73$ for V4e and $P = 0.85$ for the smaller targets).

Table 3. Test–Retest Variability for GVFs and OVFs

	Test–Retest Variability for Solid Angle Measures			
	GVF		OVF	
Parameter	V4e	Smaller-Target Isopters	V4e	Smaller-Target Isopters
All participants, *n*	27	26	27	24
Median, %	9.7	8.7	12.7	8.9
Minimum, %	0.7	0.0	0.3	0.0
Maximum, %	78	128	95	185
Participants aged ≤17 years old, *n*	9	9	9	7
Median, %	6.4	11.4	9.7	5.9
Minimum, %	2.5	0.1	0.3	3.1
Maximum, %	11.7	128	22.6	43.8
Participants aged ≥18 years old, *n*	18	17	18	17
Median, %	12.3	7.6	14.2	18.1
Minimum, %	0.7	0	0.3	0
Maximum, %	78	111	95	185

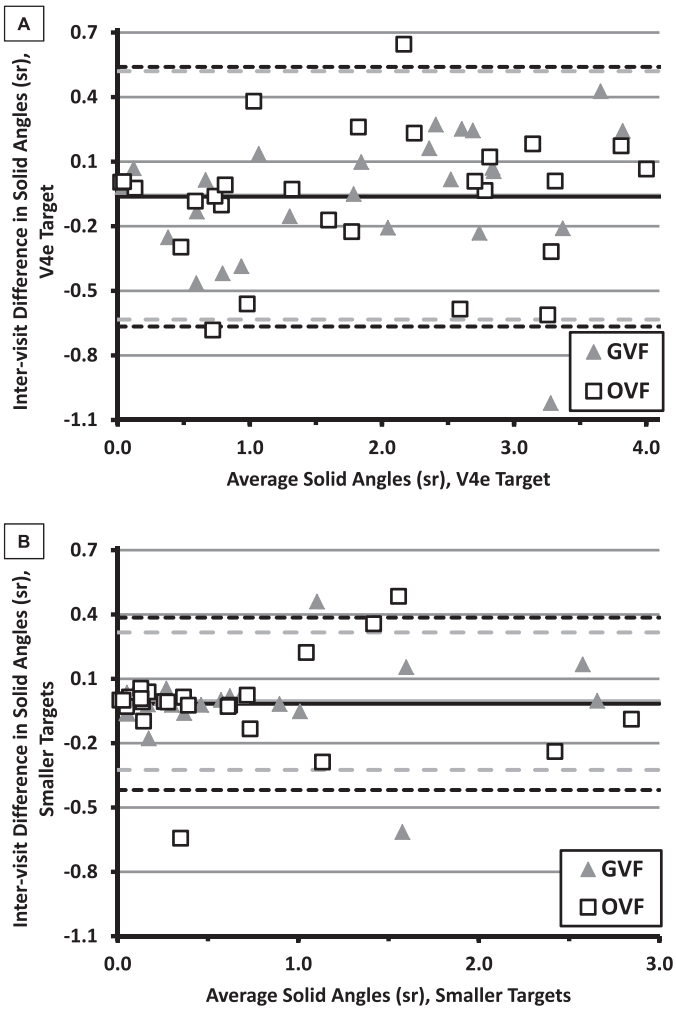

Figure 4. Bland-Altman Plots: difference in solid angles (Visit 1 – Visit 2) as a function of average solid angle for the V4e isopter (A) and for the smaller-target isopters (B). Results for each participant were calculated separately for GVFs (*triangles*) and for OVFs (*squares*). The *solid lines* (GVFs, *gray*; OVFs, *black*) show the means of the intervisit differences, whereas the *dashed lines* (GVFs, *gray*, *long dashes*; OVFs, *black*, *shorter dashes*) indicate the CR95 values. Note that the same y-axis range is used in both panels, but the x-axes differ.

The median pediatric variability values were smaller than the adult values for all conditions except the GVFs with the smaller targets, and an unpaired *t*-test comparing the set of pediatric variabilities (using the data from both perimeters and both target sizes) to the set of adult variabilities showed significantly smaller values for the pediatric group ($P = 0.03$). However, caveats must be noted regarding the wide range of values within each group, the small numbers of participants, and the tendency for the older participants to show smaller VF areas (see below).

The majority (>75%) of individual-participant variability values were below 30% for both the V4e and smaller targets, but the ranges of variabilities for the smaller targets were larger than those for the V4e targets (Table 3). However, *t*-tests did not show significant differences between the participants' variabilities for the two target-size groups, for either GVFs or OVFs (paired *t*-tests, $P = 0.28$ for GVFs and $P = 0.20$ for OVFs). Therefore, although there were more examples of extremely large variability when participants were tested with the smaller targets (with one OVF value, in particular, over 180%), the group variability did not differ significantly based on target size.

Bland-Altman plots[23] are used to examine whether response variability depends on the value of an outcome measure. The differences in solid angle between Visit 1 and Visit 2 (Visit 1 minus Visit 2) for each participant for the V4e and smaller-target isopters are shown in Figures 4A and 4B, respectively. In both panels, the differences are graphed as a function of the participant's average solid angle for the given target size (GVFs and OVFs averaged, separately, across the two visits).

The solid lines in Figure 4 indicate the means of the intervisit differences per method; the dashed lines show the values of the 95% coefficient of repeatability (CR95: ±1.96 times the standard deviation of the differences) per method. The fact that the means are near zero suggests that there was little or no practice effect from the first to second visit. For the V4e targets, the CR95 values for the two perimetry methods (0.58 for GVFs and 0.60 for OVFs) were very similar, consistent with similar variability for the two perimeters. The smaller-target CR95 values for the two perimetry methods (0.32 for GVFs and 0.40 for OVFs) were almost as close together as those for the V4e targets.

An analysis of variance of the solid angles per participant (averaged across visits), as a function of participant age, showed a trend to decreasing field size with increasing age; the relationship was significant for the V4e targets on both perimeters ($P \leq 0.02$; Supplementary Fig. S2) but not for the smaller targets ($P \geq 0.09$). To explore the possible effect of participant age on test–retest variability, scatterplots were generated by plotting the percent test–retest variability against age (Fig. 5). There were slight trends to higher variabilities with increasing age of the participants for the V4e targets on both perimeters and for the smaller-target GVFs, but none of the analysis of variance *P* values were less than 0.05 ($P = 0.31$, 0.20, and 0.89, for the GVFs for the V4e target,

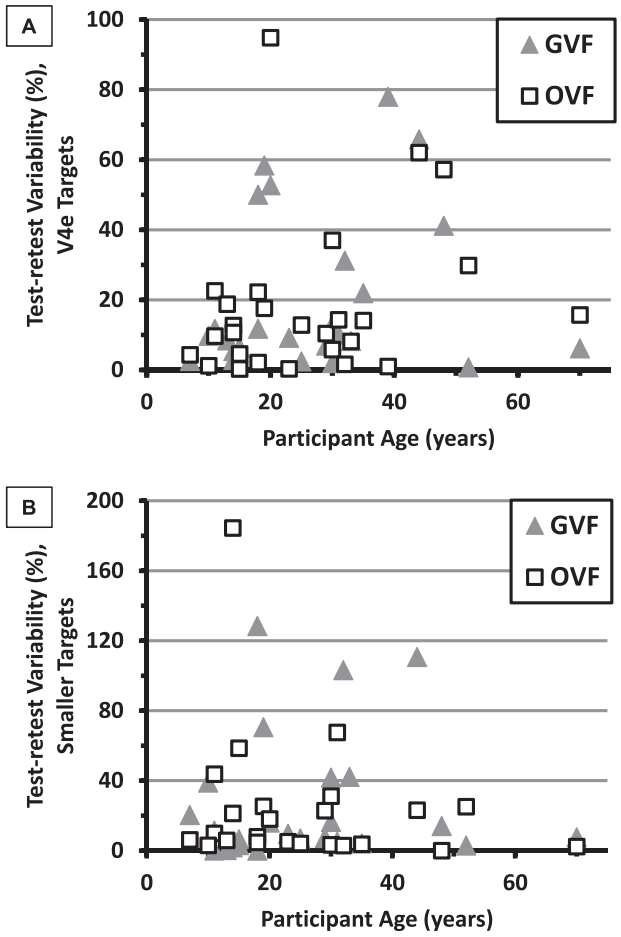

Figure 5. Percent test–retest variability as a function of participant age for the V4e target (A) and smaller targets (B). The GVF results are represented by *triangles* and the OVF results by *open squares*.

OVFs for the V4e target, and GVFs for smaller targets, respectively). Variability for the OVF smaller targets showed a nonsignificant decrease with increasing participant age ($P = 0.32$). Therefore, the present study did not demonstrate a strong dependence of test–retest variability on participant age.

The VF variabilities were also compared to the subjects' logMAR visual acuities (data not shown). All of the resultant P values were larger than 0.05 ($P =$ 0.13, 0.44, 0.41, and 0.61 for the GVF V4e target, OVF V4e target, GVF smaller targets, and OVF smaller targets, respectively), indicating that there was no significant correlation between visual acuity and test–retest variability.

Reaction Times Measured With Octopus SKP

The Octopus reaction time test was not attempted on every participant and could not be performed on participants with very small fields, so values are available for at least one visit (usually both) for only 23 of the participants. For their total of 43 measures, the median reaction time was 297 milliseconds. There was a very wide range of reaction times (from 145 to 1,957 milliseconds), as has been seen previously.[24] For the 20 participants with OVF reaction times at both visits in the present study, a t-test showed no significant difference between the reaction times measured at each visit ($P = 0.61$), suggesting that there was not a significant learning effect on response times.

Nonetheless, there were four participants who had very different reaction times at the two visits: participant B3's reaction time was 887 milliseconds faster at Visit 2, whereas the reaction times for participants B6, B9, and B10 were 341 to 493 milliseconds slower at Visit 2. These differences in reaction times might be expected to cause substantial changes in OVF size (enlarged OVFs for participant B3, with faster responses, and smaller OVFs for the other three). However, participant B3's V4e isopter was smaller, not larger, at Visit 2, with little change for the smaller-target isopter, and both of participant B9's isopters were larger at Visit 2. Only the decreased sizes of the smaller-target isopters for participants B6 and B10 were consistent with the predicted reaction-time effect.

The reaction times in the present study were compared against the variability in solid angle values from the OVFs. Note that the reaction times were not measured during the standard OVF mapping but as separate test measures. OVF variabilities for both the V4e targets and smaller targets separately increased as the reaction times (averaged across the two visits) increased. However, only the smaller targets showed a significant effect of reaction times on variability ($P =$ 0.03 for smaller targets, $P = 0.28$ for the V4e targets). This suggests that subjects with slow responses to the small targets tended to have greater test–retest variability (but that was largely determined by a small number of participants with long reaction times).

Comparison of Octopus-Generated VF Square-Degrees With Manually Digitized Solid Angles

Numerical summaries of VF images are necessary if the VFs are to be quantitatively compared across time. As Octopus perimeters can calculate VF sizes in deg^2, it is of interest to know how well those deg^2

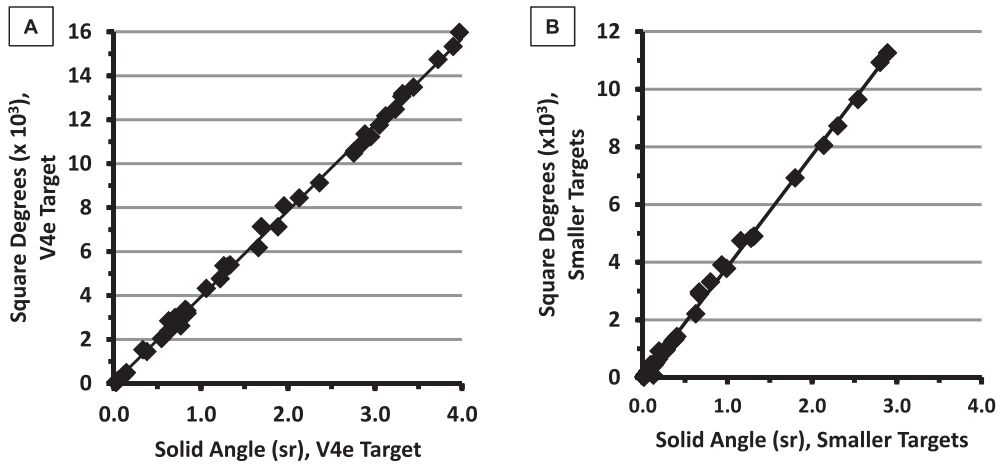

Figure 6. Retinal area (deg^2) values generated by the Octopus perimeters compared with the solid angle (sr) values from digitization of the same visual fields (V4e results in panel A). The *solid lines* show the linear regression fits.

values match the solid angle values in the present study. In Figure 6, the Octopus deg^2 values are plotted against the corresponding OVF solid angles that we derived with on-screen digitization software.

The r^2 values relating OVF deg^2 to the solid angles were virtually equal to 1.0 ($r^2 = 0.998$ for both the V4e targets and [separately] the smaller targets), indicating excellent correlation between automatically generated VF areas in deg^2 and the manually digitized values in steradians obtained from OVF scans.

Examiner Ratings of VF Performance

As the participants underwent testing on each perimeter, the examiners rated them on four factors: fixation, cooperation, fatigue, and the presence of participant-reported photopsias. In a deviation from the protocol, participant A5 and all 10 participants at Site B were only rated once per visit, rather than once per VF test, leaving 17 participants with digitizable VFs who had ratings on both tests per visit (participant A4 only had ratings for Visit 2). All performance ratings for those participants, without averaging between visits, are summarized in Table 4.

There were no ratings of 1 assigned to any of the participants, which is appropriate because a 1 in any category indicated that the participant was unable to complete one or more of the isopters during that test. Photopsias were apparently not a major impediment to the tests, as only about 12% of the participants were in the "photopsias interfering" classifications (all with ratings of 3). Fixation losses were also low and comparable between the two perimeters (6.1% and 6.3% of GVF and OVF tests, respectively, had a rating of 3), and cooperation was generally reported to be high (>72% of the ratings were a 5 for both perimeters). Over half of the participants reported some fatigue (or were observed to display fatigue or sleepiness) during the tests, but the percentage of

Table 4. Examiners' Ratings of Participants' Visual Field Performances on Four Factors, for the 17 Participants Rated Separately on GVFs and OVFs

	Rating-Scale Scores (%) ($N = 34$[a])							
	Fixation		Cooperation		Fatigue		Photopsias	
Rating	GVF	OVF	GVF	OVF	GVF	OVF	GVF	OVF
5	63.6	62.5	72.7	78.8	45.5	45.5	60.6	57.6
4	30.3	31.3	21.2	18.2	27.3	36.4	27.3	30.3
3	6.1	6.3	6.1	0.0	21.2	15.2	12.1	12.1
2	0.0	0.0	0.0	3.0	6.1	3.0	0.0	0.0
1	0.0	0.0	0.0	0.0	0.0	0.0	0.0	0.0

[a] There were no Visit 1 ratings for participant A4, and no Visit 1 OVF fixation-rating for A3, so $n = 33$ for all conditions except OVF-fixation, for which $n = 32$.

fatigue ratings less than 5 was the same for both tests (54.5%). The fact that there were more fatigue ratings of 4 for OVFs than GVFs and more ratings of 3 for GVFs than for OVFs, suggests that performing the GVFs may have been somewhat more tiring than the OVFs. An exploration of the subject variabilities for those subjects from Table 4 who had digitizable VFs ($n = 16$) did not show any relationships with any of the rating categories for either perimeter.

Discussion

In this study, VFs were digitized and the solid angle values were compared between repeat tests on the same perimeters across visits and between the Goldmann and Octopus tests within visits. There were no significant intervisit differences between the GVFs or between the OVFs. Furthermore, there were no significant differences between the solid angles for the OVFs and GVFs for the V4e targets or for the smaller targets, although there was a trend toward the OVF solid angles being slightly larger than those of the GVFs for the smaller targets. These findings are consistent with reports in the literature that GVFs tend to be somewhat smaller than the corresponding OVFs,[3,6] particularly for small, dim targets, perhaps because of the faster and/or more variable target speeds in Goldmann perimetry.[3]

Ideally, a patient or clinical trial participant would be tested repeatedly on the same type of kinetic perimeter. However, the present results suggest that solid angle values for isopters mapped on an Octopus should not be very different from those mapped on a Goldmann perimeter by a highly qualified examiner. Therefore, an individual's VFs could continue to be followed across disease progression (with or without treatment), at least approximately, despite a change in perimeter from Goldmann to Octopus. In addition, based on their qualitative study with visually impaired participants, Rowe and Rowlands[2] reported that "Octopus perimetry detected the presence of all visual field defects with strong agreement in comparison to Goldmann perimetry for type and location of defect," in their group of patients, most of whom had been diagnosed with damage to the posterior visual pathway. Our results resembled those of Rowe and Rowland in that the within- and between-visit VFs/participant generally showed similar shapes and similar locations (to the left or right of center) of any peripheral arcs or islands. With the important contribution of VFs to independent mobility,[25] it is important to track the size and location of VF regions across time.

Assuming that the same perimeter would be used throughout a given clinical trial but that different clinical trials might not all use the same perimeter, it is important to examine the test–retest variability in VFs for both types of perimeters. This study showed that test–retest variability was quite low and did not differ significantly between the Goldmann and Octopus perimeters, for either the V4e or smaller targets. Note that the use of SKP did not produce significantly lower variability values, as might have been predicted due to the standardized target movements[26] and the decreased likelihood of experimenter bias.[3] However, highly experienced perimetrists conducted the examinations, and the fact that the variability on SKP was not higher is promising for future trials as Goldmann perimeters are phased out.

There are relatively few published papers on SKP testing in children, particularly children with any form of vision impairment. Our results extend the variability study results of Patel et al.[9] They found that normally sighted children as young as age 5 can perform reliable VF tests and that among the children with "good" performance at both visits (as rated by an expert examiner), neither the GVFs nor OVFs showed statistically significant differences in area between visits. Our inclusion of some children with severe IRDs allows us to answer the critically important question about whether reliable VFs can be obtained in such children. Our results indicate that SKP testing is not only possible in children with vision loss but, in fact, generates similar results to GVF testing, with very good test–retest reliability for both test instruments. That is a particularly relevant conclusion for proposed clinical trials in which children with vision loss (e.g., due to IRDs) might be tested repeatedly with kinetic perimetry. To strengthen the present findings, we recommend that a larger number of young participants, with a wide range of vision loss, be tested.

The very close correlation between the deg^2 values generated by the Octopus perimeters and the digitized steradian values for the same OVFs suggests that VF analyses from the Octopus could proceed without manual digitizing. That is beneficial as such digitizing is not routinely available and even if it is, it is time-consuming and may introduce further variability (i.e., human error) into the measurements.[18] However, in some situations, it may be beneficial to not only provide solid angles in steradians as a summary outcome per isopter but also the mm^2 of retina (log

retinal area), as that has been demonstrated to be a meaningful measure of VF loss progression in retinitis pigmentosa.[27] Octopus perimeters do not currently provide mm^2 measurements for the isopters, but the digitization program does.

Previous studies[1,24] demonstrated that reaction times impact the sizes of measured OVFs, although these studies suggested that reaction times should not normally cause clinically significant differences. Increased reaction times were also associated with increased VF size variability, at least within a given participant's same-day repeated OVFs.[24] In the present study, linear regressions of VF variability versus reaction times only showed a significant effect for the smaller targets. The reaction times for some of our participants differed by hundreds of milliseconds between visits.

Ross et al.[17] measured GVF test–retest variability in participants with retinitis pigmentosa (tested by the same examiner) and reported variability values of about 12% but found values ranging from 0% to 50%. The same-day GVF variabilities in a study by Bittner et al.[28] for adults with retinitis pigmentosa were around 20% or 25%. However, that was after the authors excluded the most-extreme variabilities among their participants; the authors advocated that such highly variable participants should be screened out during the early pretreatment stage of a clinical trial. Bittner et al. noted that their revised variabilities were similar to the values of 22% for a significant decrease and 29% for a significant increase in GVF diameter derived by Berson et al.[29] for their 32 children and adults with retinitis pigmentosa. More recently, Roman et al.[30] reported corresponding values of −44% to +77% for their GVF study in participants with documented *RPE65* mutations. The median variabilities for the solid angles in the present study were approximately 9% to 13% but with a range of 0% to 185% for this group of participants with assorted baseline VF sizes. Differences in timing, test techniques, measurement units, and patient samples complicate attempts to compare variabilities across all of these studies. Finally, Bittner et al.[28] reported that variability tended to be higher when the V4e field area was less than 10 mm^2 (VFs with diameters less than 14 degrees) and when peripheral islands were included in the VF area. Those factors were not examined systematically in the present study, although the results in Figure 4 are not consistent with very small fields (a fraction of a steradian) being associated with large intervisit size differences.

Finally, one could question the utility of perimetry (Goldmann or SKP) in an age when multiple other technical measures (such as functional magnetic resonance imaging) are available. VFs continue to represent a fundamental test method in ongoing clinical trials (see multiple IRD trials on https://www.centerwatch.com) and in the clinical categorization of patients with newly identified genetic mutations (e.g., Ref. 16). Although several optical coherence tomography (OCT) parameters have been studied as outcome measures (e.g., the width of the ellipsoid zone[31]), OCT imaging on most machines does not reach into the mid- and far-periphery,[32] which is of interest in IRDs. Finally, with the Food and Drug Administration's stated focus now on "structure–function correlations,"[33] VFs (function) will continue to be of value even with an increased use of OCT imaging (structure).

Conclusions

Expanding beyond pediatric studies with visually normal children, this study demonstrated that Octopus SKP can be successfully and reliably performed in children with IRDs. In both children and adults, the Octopus SKP results were generally quite similar to those from Goldmann perimetry in terms of solid angles, although there was a trend to slightly larger solid angles for OVFs than GVFs when mapping with small targets. Test–retest variability, over an interval of about 1 week, did not differ significantly between the two perimetric methods for V4e targets or for smaller targets. Altogether, these results indicate that SKP on Octopus perimeters provides a viable alternative to Goldmann perimetry in clinical trials and clinical care involving children and adults with IRDs.

Acknowledgments

The authors thank the patients and families for their participation. The authors also wish to thank Retinagenix for financial support to cover the publication charge for this article.

This study was funded by QLT Inc., of Vancouver, Canada. QLT contracted the three research centers and authors CSB and RAS to perform the research activities.

Author DGB received Foundation Fighting Blindness and NIH funding R01 09076. Author RKK was

funded by the Foundation Fighting Blindness Canada and the Canadian Institutes for Health Research. Author AKB received NIH funding K23 EY018356. Author GD receives royalties from the visual-field digitization program, when it is used in commercial studies.

Presented at the Association for Research in Vision and Ophthalmology annual meeting in Orlando, FL, May 2014.

Disclosure: **C.S. Barnes**, QLT Inc. (C); **R.A. Schuchard**, QLT Inc. (C); **D.G. Birch**, QLT Inc. (F); **G. Dagnelie**, QLT Inc. (F), Johns Hopkins (P); **L. Wood**, None; **R.K. Koenekoop**, QLT Inc. (F); **A.K. Bittner**, QLT Inc. (C)

References

1. Vonthein R, Rauscher S, Paetzold J, et al. The normal age-corrected and reaction time-corrected isopter derived by semi-automated kinetic perimetry. *Ophthalmology*. 2007;114:1065–1072.
2. Rowe FJ, Rowlands A. Comparison of diagnostic accuracy between Octopus 900 and Goldmann kinetic visual fields. *Biomed Res Int*. 2014: 214829.
3. Nowomiejska K, Vonthein R, Paetzold J, Zagorski Z, Kardon R, Schiefer U. Comparison between semiautomated kinetic perimetry and conventional Goldmann manual kinetic perimetry in advanced visual field loss. *Ophthalmology*. 2005;112:1343–1354.
4. Wilscher S, Wabbels B, Lorenz B. Feasibility and outcome of automated kinetic perimetry in children. *Graef Arch Clin Exp Ophthalmol*. 2010; 248:1493–1500.
5. Pineles SL, Volpe NJ, Miller-Ellis E, et al. Automated combined kinetic and static perimetry: an alternative to standard perimetry in patients with neuro-ophthalmic disease and glaucoma. *Arch Ophthalmol*. 2006;124:363–369.
6. Ramirez AM, Chaya CJ, Gordon LK, Giaconi JA. A comparison of semiautomated versus manual Goldmann kinetic perimetry in patients with visually significant glaucoma. *J Glaucoma*. 2008;17:111–117.
7. Bevers C, Blanckaert G, Van Keer K, Fils JF, Vandewalle E, Stalmans I. Semi-automated kinetic perimetry: Comparison of the Octopus 900 and Humphrey visual field analyzer 3 versus Goldmann perimetry. *Acta Ophthalmol*. 2018;97: e499–e505. https://doi.org/10.1111/aos.13940.
8. Patel DE, Cumberland PM, Walters BC, Russell-Eggitt I, Rahi JS; OPTIC study group. Study of Optimal Perimetric Testing in Children (OPTIC): feasibility, reliability and repeatability of perimetry in children. *PLoS One*. 2015;10:e0130895.
9. Nowomiejska K, Brzozowska A, Koss MJ, et al. Quantification of the visual field loss in retinitis pigmentosa using semi-automated kinetic perimetry. *Curr Eye Res*. 2016;41:993–998.
10. Nevalainen J, Paetzold J, Krapp E, Vonthein R, Johnson CA, Schiefer U. The use of semi-automated kinetic perimetry (SKP) to monitor advanced glaucomatous visual field loss. *Graefes Arch Clin Exp Ophthalmol*. 2008;246:1331–1339.
11. Parker MA, Choi D, Erker LR, et al. Test-retest variability of functional and structural parameters in patients with Stargardt disease participating in the SAR422459 gene therapy trial. *Trans Vis Sci Tech*. 2016;5:10.
12. Nowomiejska K, Jedrych M, Brzozowska A, et al. Relationship between the area of isopters and Vigabatrin dosage during two years of observation. *BMC Ophthalmol*. 2014;14:56.
13. Hirasawa K, Shoji N. Learning effect and repeatability of automated kinetic perimetry in healthy participants. *Curr Eye Res*. 2014;39:928–937.
14. Bjerre A, Codina C, Griffiths H. Peripheral visual fields in children and young adults using semi-automated kinetic perimetry: Feasibility of testing, normative data, and repeatability. *Neuro-ophthalmology*. 2014;38:189–198.
15. Nowomiejska K, Kiszka A, Koman-Wierdak E, et al. Analysis of visual field defects obtained with semiautomated kinetic perimetry in patients with Leber hereditary optic neuropathy. *J Ophthalmol*. 2018: 5985702.
16. Nasser F, Weisschuh N, Maffei P, et al. Ophthalmic features of cone-rod dystrophy caused by pathogenic variants in the *ALMS1* gene. *Acta Ophthalmol*. 2018;96:e445–e454.
17. Ross DF, Fishman GA, Gilbert LD, Anderson RJ. Variability of visual-field measurements in normal subjects and patients with Retinitis pigmentosa. *Arch Ophthalmol*. 1984;102:1004–1010.
18. Dagnelie G. Conversion of planimetric visual field data into solid angles and retinal areas. *Clin Vis Sci*. 1990;5:95–100.
19. Barry MP, Bittner AK, Yang L, Marcus R, Iftikhar MH, Dagnelie G. Variability and errors

of manually digitized Goldmann visual fields. *Optom Vis Sci*. 2016;93:720–730.
20. Talib M, Dagnelie G, Boon CJF. Recording and analysis of Goldmann kinetic visual fields. In: Boon C, Wijnholds J, eds. *Retinal Gene Therapy*. *Methods in Molecular Biology*, vol 1715. New York, NY: Humana Press; 2018:327–338.
21. World Health Organization. Youth and health risks. Report by the Secretariat 2011. Available at: http://apps.who.int/gb/ebwha/pdf_files/WHA64/A64_25-en.pdf. Accessed April 27, 2018.
22. Schulze-Bonsel K, Feltgen N, Burau H, Hansen L, Bach M. Visual acuities "hand motion" and "counting fingers" can be quantified with the Freiburg visual acuity test. *Invest Ophthalmol Vis Sci*. 2006;47:1236–1240.
23. Bland JM, Altman DG. Statistical methods for assessing agreement between two methods of clinical measurement. *Lancet*. 1986;1:307–310.
24. Nowomiejska K, Vonthein R, Paetzold J, Zagorski Z, Kardon R, Schiefer U. Reaction time during semi-automated kinetic perimetry (SKP) in patients with advanced visual field loss. *Acta Ophthalmol*. 2010;88:65–69.
25. Authié CN, Berthoz A, Sahel JA, Safran AB. Adaptive gaze strategies for locomotion with constricted visual field. *Front Hum Neurosci*. 2017;11:387.
26. Dolderer J, Vonthein R, Johnson CA, Schiefer U, Hart W. Scotoma mapping by semi-automated kinetic perimetry: the effects of stimulus properties and the speed of subjects' responses. *Acta Ophthalmologica Scand*. 2006;84:338–344.
27. Massof RW, Dagnelie G, Benzschawel T, Palmer RW, Finkelstein D. First order dynamics of visual field loss in retinitis pigmentosa. *Clin Vis Sci*. 1990;5:l–26.
28. Bittner AK, Iftikhar MH, Dagnelie G. Test-retest, within-visit variability of Goldmann visual fields in retinitis pigmentosa. *Invest Ophthalmol Vis Sci*. 2011;52:8042–8046.
29. Berson EL, Sandberg MA, Rosner B, Birch DG, Hanson AH. Natural course of retinitis pigmentosa over a three-year interval. *Am J Ophthalmol*. 1985;99:240–251.
30. Roman AJ, Cideciyan AV, Schwartz SB, Olivares MB, Heon E, Jacobson SG. Intervisit variability of visual parameters in Leber congenital amaurosis caused by *RPE65* mutations. *Invest Ophthalmol Vis Sci*. 2013;54:1378–1383.
31. Birch DG, Locke KG, Wen Y, Locke KI, Hoffman DR, Hood DC. Spectral-domain optical coherence tomography measures of outer segment layer progression in patients with X-linked retinitis pigmentosa. *JAMA Ophthalmol*. 2013;131:1143–1150.
32. Kolb JP, Klein T, Kufner CL, Wieser W, Neubauer AS, Huber R. Ultra-widefield retinal MHz-OCT imaging with up to 100 degrees viewing angle. *Biomed Opt Express*. 2015;6:1534–1552.
33. Csaky K, Ferris F III, Chew EY, Nair P, Cheetham JK, Duncan JL. Report from the NEI/FDA Endpoints Workshop on age-related macular degeneration and inherited retinal diseases. *Invest Ophthalmol Vis Sci*. 2017;58:3456–3463.